Latin American Applied Research 34:229-240 (2004)

COSSERAT CONTINUA-BASED MICRO PLANE MODELLING. THEORY AND NUMERICAL ANALYSIS

G. ETSE† and M. NIETO‡

†*CONICET and Center for Numerical and Computational Methods in Engng., University of Tucumán, Roca 1800, 4000-Tucumán, ARGENTINA. getse@herrera.unt.edu.ar*
‡*Civil Engng. Department, University of Santiago del Estero, 4200 – Sgo. del Estero, ARGENTINA*

***Abstract*—** **The well-known micro plane theory is extended to account for micro rotations and couple stresses in the framework of the micro polar Cosserat continua. The main purpose is to obtain reliable macroscopic constitutive equations and models for engineering materials like concrete and other composites based on available and precise information of their complex microstructure. The proposed macroscopic descriptions account also for anisotropic material response behavior by means of the well-developed micro plane concept applied within a micro polar continuum setting. For the formulation of the micro polar-based micro plane theory a thermodynamically consistent approach is considered, whereby the main assumption is the integral relation between the macroscopic and the microscopic free energy as advocated by Carol** *et al.* **(2001) and Kuhl** *et al.* **(2001). Thereby, the micro plane laws are chosen such that the macroscopic Clausius-Duhem inequality is fully satisfied. This theoretical framework is considered to derive both elastic and elastoplastic micro polar micro plane models. Numerical predictions of the uniaxial tensile and simple shear tests in plane strain conditions obtained with a micro polar micro plane elastoplastic model are also presented and contrasted to the corresponding predictions of the classical micro polar elastoplastic model.**

***Keywords*—** plasticity, micropolar, microplane, localized failure.

I. INTRODUCTION

One of the most successful constitutive theories for the analysis of the engineering materials is the micro plane theory which is characterized by three relevant features. On one hand, it incorporates microscopic information in the macroscopic material formulation in a natural way. On the other hand, very simple constitutive equations at the micro plane level lead to highly accurate macroscopic predictions of material behaviors. The third relevant aspect of the micro plane theory is its capacity to model anisotropic material behaviors. Actually, this was one of the most important objectives of the original proposal by Taylor (1938) which is based on the definition of fully independent uniaxial stress-strain relations on several planes of the material.

Based on Taylor's idea the micro plane theory was then pioneered by Bazant and Gambarova (1984), Bazant (1984) and Bazant and Oh (1985, 1986).

For the formulation of the uniaxial stress-strain relations on the micro planes, two different approaches may be considered, whereby the static or the kinematic constraint require that either the stresses or the strains on each micro plane are the resolved components of their macroscopic counterparts. The static constraint was extensively used until the first application of the micro plane theory to continuum damage mechanics and to cohesive-frictional materials by Bazant and Gambarova (1984) and Bazant (1984). It was in those works were the name micro plane appeared for the first time instead of the original terminology slip theory which was related to the plastic behavior assumption on slip planes by Taylor and other authors like Batdorf and Budianski (1949). The potentials of the micro plane theory for describing non linear response behaviors of engineering cohesive-frictional materials like concrete were extensively demonstrated in the first contributions by Bazant and coauthors related with the micro plane theory and, more recently, in the works by Bazant and Prat (1988), Carol *et al.* (1991, 1992) and Carol and Bazant (1997), among many others.

Recently, the lack of a thermodynamically consistent approach for deriving micro plane-based constitutive formulations was advocated by Carol *et al.* (2001) who demonstrated that the satisfaction of the second law of thermodynamics could generally not be guaranteed. To solve this fundamental shortcoming they proposed a method for deriving micro plane constitutive formulations within a thermodynamically consistent framework by means of the incorporation of a microscopic free Helmholtz energy on every micro plane. This concept was successfully extended for inelastic material behavior such as damage and plasticity by Kuhl *et al.* (2001). However, both this work as well as the previous one by Carol *et al.* (2001) were concerned with classical Boltzmann continua (elastic and inelastic).

Despite the advantages of the micro plane theory and the considerable progress of the related models since the original Taylor's proposal, it still has open questions and the most relevant one is how to incorporate more detailed microscopic information in the global constitutive equations to be able to reproduce particular material behaviors.

In this work the thermodynamically consistent approach to derive micro plane models is further extended for micro polar continua in the spirit of Cosserat and Cosserat (1909). The main aim is to enrich the microscopic kinematic and strength features of the micro plane formulation so as to reproduce particular and more complex behaviors of the internal structure of composite quasi-brittle materials like concrete whereby the presence of aggregates may contribute to the development of microrotations in characteristic planes during load histories beyond the elastic limit.

The second motivation of the micro polar micro plane theory in this work is related to the regularization of the post peak predictions of the smeared crack concept. In this sense, the incorporation of the micro polar length scale at the microscopic level leads to an intrinsically non local micro plane constitutive relation when the additional degrees of freedom of micro polar continua are activated. This characteristic length accounts for mesh objectivity during FE simulations of softening behaviors.

After revising the most relevant equations of the Cosserat continuum in the next section, the micro plane theory is extended to the micro polar continuum in section 3. Thereby, both the static and the kinematic constraint are redefined to include the macroscopic couple stress and the macroscopic curvature projections at micro planes, respectively. Section 4 is concerned with the hemispherical integrations which are required for the closed form formulation of some micro polar micro plane models. In section 5 the attention focuses on the method for deriving micro polar micro plane constitutive equations. Section 6 refers to the application of the proposed thermodynamically consistent method to the formulation of general 3D linear elastic models. In section 7, elastoplastic constitutive equations are derived both for the general case and for the von Mises type model. Finally, in section 8 the numerical predictions of the micro polar micro plane elastoplastic von Mises model for the uniaxial tensile and simple shear tests are presented and compared with those of the classical micro polar elastoplastic von Mises model. The comparative results illustrate the fundamental differences between the predictions of the micro polar micro plane and the classical micro polar models. Moreover, the results also demonstrate the potentials of the proposed thermodynamically consistent approach to derive constitutive models based on enriched kinematic and strength properties at the microscopic level and thus allowing for computational simulations of complex anisotropic response behavior of engineering materials.

II. FUNDAMENTALS OF COSSERAT THEORY

In this section the relevant equations of the micro polar Cosserat theory are presented. This theory was proposed by Cosserat and Cosserat(1909) at the beginning of the twenty century. However, it was only in the last decades that a revival of this theory took place through the contributions of many different authors who analyzed the benefits of the micro polar theory from different points of view. Among others, the most prominent work in this regard was made by Eringen (1968) who presented a detailed analysis of elastic micro polar continua and of their mechanical features. The first application of the micro polar continuum in non-linear computational solid mechanics took place at the end of the 1980's in the works by Mühlhaus (1989) and de Borst (1991) who analyzed the potentials of the elastoplastic micro polar constitutive theory to regularize the predictions of post-peak response behaviors of structural systems within the theoretical framework of the smeared-crack approach. In the same line, Steinmann and Willam (1991), Willam and Dietsche (1992), Sluys (1992) and Willam *et al.* (1995) analyzed the localization indicators and localization properties of nonlinear micro polar continua.

A. Stresses at Macro Level

The stress components in micro polar continua defined in the general 3D domain $\mathcal{B}$ follow from the quasi-static form of linear and angular momentum which reads (omitting body forces and body couples for simplicity)

$$\begin{aligned} \mathrm{div}\boldsymbol{\sigma}^t &= \mathbf{0} \\ \mathrm{div}\boldsymbol{\mu}^t + \boldsymbol{e} : \boldsymbol{\sigma} &= \mathbf{0} \end{aligned} \tag{1}$$

whereby $\boldsymbol{\mu}$ is a non symmetric second order tensor which represents the couple stresses of the micro polar continuum. The local equilibrium equations of the classical continuum and the corresponding typical symmetric form of the stress tensor $\boldsymbol{\sigma}$ are restored when $\mathrm{div}\boldsymbol{\mu}^t = \mathbf{0} \rightarrow \boldsymbol{e} : \boldsymbol{\sigma} = \mathbf{0}$. Here e denotes the third order permutation tensor.

B. Strain and Curvature at Macro Level

The deformation of the micro polar continuum is a consequence of the simultaneous action of two types of local or micro motions: the classical or translatory ones, represented by the displacement field $\boldsymbol{u}$, and the pointwise rotations characterized by the first order tensor $\boldsymbol{\omega}$. This enriched motion field leads to the following strain measures

$$\begin{aligned} \boldsymbol{\epsilon} &= \nabla_x \boldsymbol{u} - \boldsymbol{\Omega} \\ \boldsymbol{\kappa} &= \nabla_x \boldsymbol{\omega} \end{aligned} \tag{2}$$

with $\boldsymbol{\Omega} = -\boldsymbol{e} \cdot \boldsymbol{\omega}$. Here $\boldsymbol{\epsilon}$ represents the non-symmetric micro polar strain tensor and $\boldsymbol{\kappa}$ is the micro curvature tensor which takes into account the differential changes of the micro rotations in the neighborhood of a point.

The second order strain tensor may finally be decomposed into a symmetric and skew-symmetric contribution $\boldsymbol{\epsilon} = \boldsymbol{\epsilon}^{sym} + \boldsymbol{\epsilon}^{skw}$ with

$$\begin{aligned} \boldsymbol{\epsilon}^{sym} &= \frac{1}{2}[\nabla_x \boldsymbol{u} + \nabla_x^t \boldsymbol{u}] \\ \boldsymbol{\epsilon}^{skw} &= \frac{1}{2}[\nabla_x \boldsymbol{u} - \nabla_x^t \boldsymbol{u}] + \boldsymbol{e} \cdot \boldsymbol{\omega} \end{aligned} \tag{3}$$

III. THE MICRO PLANE THEORY

In the micro plane theory the macro-mechanical response behavior of materials is controlled by constitutive equations of characteristic planes or micro planes by means of the static or the kinematic constraint, requiring that either the stresses or the strains on each micro plane, respectively, can be derived by projections of their macroscopic counterparts.

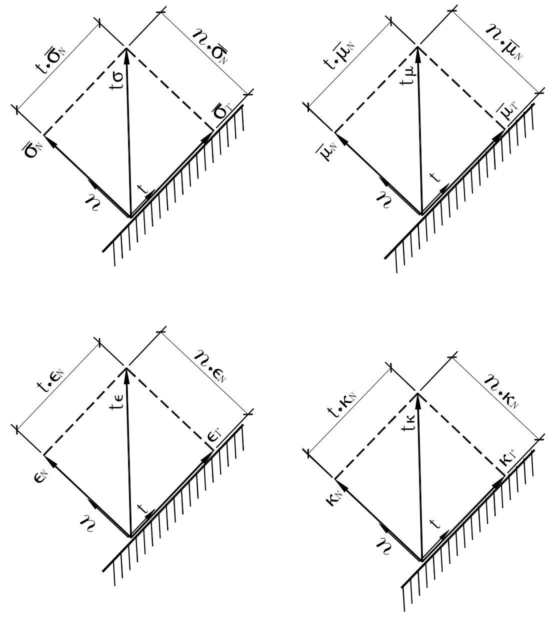

Figure 1: Micro plane normal and tangent components of the strain and curvature tensors

A. Stresses and Couple Stresses at Micro Planes

For the case of the static constraint the stress and couple stress (traction) vectors on each micro plane, see Fig. 1, are given by premultiplication with the micro plane normal vector $\boldsymbol{n}$, i.e.

$$\bar{\boldsymbol{t}}_\sigma = \boldsymbol{n} \cdot \boldsymbol{\sigma} \qquad \bar{\boldsymbol{t}}_\mu = \boldsymbol{n} \cdot \boldsymbol{\mu} \tag{4}$$

The micro plane stresses and couple stresses follow as their normal and tangential components

$$\begin{aligned} \bar{\boldsymbol{\sigma}}_N = \bar{\sigma}_N \boldsymbol{n} \qquad & \bar{\boldsymbol{\mu}}_T = \bar{\boldsymbol{t}}_\mu - \bar{\boldsymbol{\mu}}_N \\ \bar{\boldsymbol{\mu}}_N = \bar{\mu}_N \boldsymbol{n} \qquad & \bar{\boldsymbol{\sigma}}_T = \bar{\boldsymbol{t}}_\sigma - \bar{\boldsymbol{\sigma}}_N \end{aligned} \tag{5}$$

and are obtained as projections of their macroscopic counterparts to the micro planes

$$\begin{aligned} \bar{\sigma}_N = \boldsymbol{N} : \boldsymbol{\sigma} \qquad & \bar{\boldsymbol{\sigma}}_T = \boldsymbol{T} : \boldsymbol{\sigma} \\ \bar{\mu}_N = \boldsymbol{N} : \boldsymbol{\mu} \qquad & \bar{\boldsymbol{\mu}}_T = \boldsymbol{T} : \boldsymbol{\mu} \end{aligned} \tag{6}$$

Here, the second and third order projection tensors $\boldsymbol{N}$ and $\boldsymbol{T}$ are defined with $[\mathsf{I}]_{ijkl} = \delta_{ik}\delta_{jl}$ the fourth order identity tensor and $\boldsymbol{n}$ the micro plane normal vector as

$$\begin{aligned} \boldsymbol{N} &= \boldsymbol{n} \otimes \boldsymbol{n} \\ \boldsymbol{T} &= \boldsymbol{n} \cdot \mathsf{I} - \boldsymbol{n} \otimes \boldsymbol{n} \otimes \boldsymbol{n} \end{aligned} \tag{7}$$

Thus, $\bar{\sigma}_N$ and $\bar{\mu}_N$ represent the normal projected stress and normal projected couple stress, respectively, while $\bar{\boldsymbol{\sigma}}_T$ and $\bar{\boldsymbol{\mu}}_T$

denote the tangential projected stress and tangential projected couple stress vectors. Note however that these projected components of the macroscopic stress and couple stress tensors are in general different from those derived from constitutive equations at the micro planes, that we shall denote as $\sigma_N,\ \boldsymbol{\sigma}_T,\ \mu_N,\ \boldsymbol{\mu}_T$ in the sequel.

The micro plane normal and tangential stresses and couple stresses may be further decomposed into symmetric and skew-symmetric parts according to the usual decomposition strategy in a micro polar continuum. Nevertheless, since we shall not use explicitly the static constraint in the sequel, we refrain from doing so.

B. Strains and Curvatures at Micro Planes

For the case of the kinematic constraint the strain and curvature vectors on each micro plane, compare Fig. 1, are given by post-multiplication with the micro plane normal vector $\boldsymbol{n}$, i.e.

$$\boldsymbol{t}_\epsilon = \boldsymbol{\epsilon}\cdot\boldsymbol{n} = \nabla_n \boldsymbol{u} - \boldsymbol{\omega}\times\boldsymbol{n};\ \boldsymbol{t}_\kappa = \boldsymbol{\kappa}\cdot\boldsymbol{n} = \nabla_n\boldsymbol{\omega} \quad (8)$$

The micro plane strains and curvatures follow as their normal and tangential components

$$\begin{aligned} \boldsymbol{\epsilon}_N &= \epsilon_N \boldsymbol{n} & \boldsymbol{\kappa}_T &= \boldsymbol{t}_\kappa - \boldsymbol{\kappa}_N \\ \boldsymbol{\kappa}_N &= \kappa_N \boldsymbol{n} & \boldsymbol{\epsilon}_T &= \boldsymbol{t}_\epsilon - \boldsymbol{\epsilon}_N \end{aligned} \quad (9)$$

These equations are valid both for the symmetric as well as for the skew-symmetric parts of the strain and curvature measures. Taking into account the following properties

$$\boldsymbol{\epsilon}^{skw}\cdot\boldsymbol{n} = -\boldsymbol{n}\cdot\boldsymbol{\epsilon}^{skw},\quad \boldsymbol{\kappa}^{skw}\cdot\boldsymbol{n} = -\boldsymbol{n}\cdot\boldsymbol{\kappa}^{skw}$$

$$\boldsymbol{\epsilon}^{sym}\cdot\boldsymbol{n} = \boldsymbol{n}\cdot\boldsymbol{\epsilon}^{sym},\quad \boldsymbol{\kappa}^{sym}\cdot\boldsymbol{n} = \boldsymbol{n}\cdot\boldsymbol{\kappa}^{sym} \quad (10)$$

the symmetric and skew-symmetric micro plane strain components in the normal and tangential directions of micro planes are then defined by

$$\begin{aligned} \epsilon_N &= \boldsymbol{N}:\boldsymbol{\epsilon}^{sym} = \boldsymbol{N}:\boldsymbol{\epsilon} \\ \boldsymbol{\epsilon}_T^{sym} &= \boldsymbol{T}:\boldsymbol{\epsilon}^{sym} = \boldsymbol{T}^{sym}:\boldsymbol{\epsilon} \\ \boldsymbol{\epsilon}_T^{skw} &= -\boldsymbol{T}:\boldsymbol{\epsilon}^{skw} = -\boldsymbol{T}^{skw}:\boldsymbol{\epsilon} \end{aligned} \quad (11)$$

while the corresponding micro plane curvature components in the normal and tangential directions of micro planes are given by

$$\begin{aligned} \kappa_N &= \boldsymbol{N}:\boldsymbol{\kappa}^{sym} = \boldsymbol{N}:\boldsymbol{\kappa} \\ \boldsymbol{\kappa}_T^{sym} &= \boldsymbol{T}:\boldsymbol{\kappa}^{sym} = \boldsymbol{T}^{sym}:\boldsymbol{\kappa} \\ \boldsymbol{\kappa}_T^{skw} &= -\boldsymbol{T}:\boldsymbol{\kappa}^{skw} = -\boldsymbol{T}^{skw}:\boldsymbol{\kappa} \end{aligned} \quad (12)$$

Here, in addition to the projection tensor $\boldsymbol{T}$ the symmetric and skew-symmetric projection tensors $\boldsymbol{T}^{sym}$ and $\boldsymbol{T}^{skw}$ with $\boldsymbol{T} = \boldsymbol{T}^{sym} + \boldsymbol{T}^{skw}$ are defined as

$$\begin{aligned} \boldsymbol{T}^{sym} &= \boldsymbol{n}\cdot\mathsf{I}^{sym} - \boldsymbol{n}\otimes\boldsymbol{n}\otimes\boldsymbol{n} \\ \boldsymbol{T}^{skw} &= \boldsymbol{n}\cdot\mathsf{I}^{skw} \end{aligned} \quad (13)$$

whereby $[\mathsf{I}^{sym}]_{ijkl} = [\delta_{ik}\delta_{jl} + \delta_{il}\delta_{jk}]/2$ and $[\mathsf{I}^{skw}]_{ijkl} = [\delta_{ik}\delta_{jl} - \delta_{il}\delta_{jk}]/2$ are the symmetric and skew-symmetric parts of the fourth order identity tensor $\mathsf{I} = \mathsf{I}^{sym} + \mathsf{I}^{skw}$.

IV. HEMISPHERICAL INTEGRATIONS

The integration properties of the micro plane normal vector $\boldsymbol{n}$ are documented e.g. in the works of by Bazant and Oh (1986) and Lubarda and Krajcinovic (1993) are applied to perform analytical integrations over the hemisphere Ω

$$\begin{aligned} \int_\Omega d\Omega &= 2\pi \\ \int_\Omega \boldsymbol{n}\otimes\boldsymbol{n}\ d\Omega &= \frac{2\pi}{3}\boldsymbol{I} \\ \int_\Omega \boldsymbol{n}\otimes\boldsymbol{n}\otimes\boldsymbol{n}\otimes\boldsymbol{n}\ d\Omega &= \frac{2\pi}{3}\left[\mathsf{I}_{vol} + \frac{2}{5}\mathsf{I}_{dev}^{sym}\right] \end{aligned} \quad (14)$$

with $[\boldsymbol{I}]_{ij} = \delta_{ij}$ the second order identity tensor and the volumetric and symmetric deviatoric fourth order projection tensors defined as

$$\mathsf{I}_{vol} = \frac{1}{3}\boldsymbol{I}\otimes\boldsymbol{I} \qquad \mathsf{I}_{dev}^{sym} = \mathsf{I}^{sym} - \mathsf{I}_{vol} \quad (15)$$

For later use the relevant products of the projection tensors $\boldsymbol{T}$ and $\boldsymbol{N}$ are given as

$$\begin{aligned} \left[\boldsymbol{T}^T\cdot\boldsymbol{T}\right]_{ijkl} &:= T_{aij}T_{akl} = n_i n_k \delta_{jl} - n_i n_j n_k n_l \\ [\boldsymbol{N}\otimes\boldsymbol{N}]_{ijkl} &= n_i n_j n_k n_l \end{aligned} \quad (16)$$

and thus integrate over the hemisphere into

$$\begin{aligned} \frac{3}{2\pi}\int_\Omega \boldsymbol{T}^T\cdot\boldsymbol{T}d\Omega &= \mathsf{I}^{skw} + \frac{3}{5}\mathsf{I}_{dev}^{sym} \\ \frac{3}{2\pi}\int_\Omega \boldsymbol{N}\otimes\boldsymbol{N}d\Omega &= \mathsf{I}_{vol} + \frac{2}{5}\mathsf{I}_{dev}^{sym} \end{aligned} \quad (17)$$

Accordingly, the relevant products of $\boldsymbol{T}^{sym}$ and $\boldsymbol{T}^{skw}$ are given as

$$\begin{aligned} \left[[\boldsymbol{T}^{sym}]^T\cdot\boldsymbol{T}^{sym}\right]_{ijkl} &= \frac{1}{4}\left[n_i n_k\delta_{jl} + n_i n_l\delta_{jk} + \delta_{il}n_j n_k + \delta_{ik}n_j n_l\right] - n_i n_j n_k n_l \quad (18) \\ \left[[\boldsymbol{T}^{skw}]^T\cdot\boldsymbol{T}^{skw}\right]_{ijkl} &= \frac{1}{4}\left[n_i n_k\delta_{jl} - n_i n_l\delta_{jk} - \delta_{il}n_j n_k + \delta_{ik}n_j n_l\right] \\ \left[[\boldsymbol{T}^{skw}]^T\cdot\boldsymbol{T}^{sym}\right]_{ijkl} &= \frac{1}{4}\left[n_i n_k\delta_{jl} + n_i n_l\delta_{kj} - \delta_{il}n_j n_k - \delta_{ik}n_j n_l\right] \end{aligned}$$

and thus integrate over the hemisphere into

$$\begin{aligned}\frac{3}{2\pi}\int_\Omega [\boldsymbol{T}^{sym}]^T\cdot\boldsymbol{T}^{sym}d\Omega &= \frac{3}{5}\mathsf{I}^{sym}_{dev} \quad (19)\\ \frac{3}{2\pi}\int_\Omega [\boldsymbol{T}^{skw}]^T\cdot\boldsymbol{T}^{skw}d\Omega &= \mathsf{I}^{skw}\\ \frac{3}{2\pi}\int_\Omega [\boldsymbol{T}^{skw}]^T\cdot\boldsymbol{T}^{sym}d\Omega &= \mathsf{O}\end{aligned}$$

V. THERMODYNAMICALLY CONSISTENT MICRO PLANE MODELLING

Based on the proposal by Carol *et al.* (2001) and Kuhl *et al.* (2001) we develop here a general formulation for thermodynamically consistent micro polar micro plane constitutive laws. The macroscopic Clausius-Duhem inequality for isothermal processes reads

$$\mathcal{D}^{mac} = \boldsymbol{\sigma}^t:\dot{\boldsymbol{\epsilon}}+\boldsymbol{\mu}^t:\dot{\boldsymbol{\kappa}}-\dot{\psi}^{mac}\geq 0 \quad (20)$$

Next, the main assumption is given by a relation between the microscopic and macroscopic free energy, compare Carol *et al.* (2001) and Kuhl *et al.* (2001)

$$\psi^{mac}=\frac{3}{2\pi}\int_\Omega \psi^{mic}d\Omega \quad (21)$$

Moreover we consider the convenient uncoupled format of the microscopic free energy dependent on strain and curvatures components ϵ_N, $\boldsymbol{\epsilon}_T^{sym}$, $\boldsymbol{\epsilon}_T^{skw}$ and κ_N, $\boldsymbol{\kappa}_T^{sym}$, $\boldsymbol{\kappa}_T^{skw}$, respectively, as well as on the sets of internal variables $\boldsymbol{q}_u$, $\boldsymbol{q}_\omega$, related with the translatory motions and rotations, respectively

$$\psi^{mic} = \underbrace{\psi_u^{mic}(\epsilon_N,\boldsymbol{\epsilon}_T^{sym},\boldsymbol{\epsilon}_T^{skw},\boldsymbol{q}_u)}_{\text{membrane energy}} + \underbrace{\psi_\omega^{mic}(\kappa_N,\boldsymbol{\kappa}_T^{sym},\boldsymbol{\kappa}_T^{skw},\boldsymbol{q}_\omega)}_{\text{bending energy}} \quad (22)$$

Thus an additive decomposition of the total microscopic free energy into a membrane energy and a bending energy was assumed. This corresponds to the particular case of micro polar response behavior where the membrane-bending coupling diminishes to zero.

The evolution law of the microscopic free energy follows from the kinematic constraint relations in Eqs.(11) to (13)

$$\begin{aligned}\dot{\psi}^{mic} &= \left[\sigma_N\boldsymbol{N}+\boldsymbol{\sigma}_T^{sym}\cdot\boldsymbol{T}^{sym}-\boldsymbol{\sigma}_T^{skw}\cdot\boldsymbol{T}^{skw}\right]:\dot{\boldsymbol{\epsilon}}\\ &+\left[\mu_N\boldsymbol{N}+\boldsymbol{\mu}_T^{sym}\cdot\boldsymbol{T}^{sym}-\boldsymbol{\mu}_T^{skw}\cdot\boldsymbol{T}^{skw}\right]:\dot{\boldsymbol{\kappa}}\\ &-\mathcal{D}_u^{mic}-\mathcal{D}_\omega^{mic} \quad (23)\end{aligned}$$

with σ_N, $\boldsymbol{\sigma}_T^{sym}$ and $\boldsymbol{\sigma}_T^{skw}$ the microscopic constitutive stresses

$$\sigma_N:=\frac{\partial\psi^{mic}}{\partial\epsilon_N};\ \boldsymbol{\sigma}_T^{sym}:=\frac{\partial\psi^{mic}}{\partial\boldsymbol{\epsilon}_T^{sym}}$$

$$\boldsymbol{\sigma}_T^{skw}:=\frac{\partial\psi^{mic}}{\partial\boldsymbol{\epsilon}_T^{skw}} \quad (24)$$

and μ_N, $\boldsymbol{\mu}_T^{sym}$ and $\boldsymbol{\mu}_T^{skw}$ the microscopic constitutive couple stresses

$$\mu_N:=\frac{\partial\psi^{mic}}{\partial\kappa_N};\ \boldsymbol{\mu}_T^{sym}:=\frac{\partial\psi^{mic}}{\partial\boldsymbol{\kappa}_T^{sym}}$$

$$\boldsymbol{\mu}_T^{skw}:=\frac{\partial\psi^{mic}}{\partial\boldsymbol{\kappa}_T^{skw}} \quad (25)$$

and $\mathcal{D}_u^{mic}$, $\mathcal{D}_\omega^{mic}$ the microscopic dissipation rate of membrane and bending type, respectively,

$$\mathcal{D}_u^{mic}:=-\frac{\partial\psi^{mic}}{\partial\boldsymbol{q}_u}\star\dot{\boldsymbol{q}}_u;\ \mathcal{D}_\omega^{mic}:=-\frac{\partial\psi^{mic}}{\partial\boldsymbol{q}_\omega}\star\dot{\boldsymbol{q}}_\omega \quad (26)$$

whereby $\star$ indicates the appropriate contraction. Recall however, that the constitutive stresses and couple stresses on the micro planes are in general different from the projected micro plane stress and couple stress components $\bar{\sigma}_N,\bar{\boldsymbol{\sigma}}_T^{sym},\bar{\boldsymbol{\sigma}}_T^{skw}$ and $\bar{\mu}_N,\bar{\boldsymbol{\mu}}_T^{sym},\bar{\boldsymbol{\mu}}_T^{skw}$ obtained by means of the static constraint.

Due to the membrane-bending decoupling assumption, the stress tensor components can be derived from that portion of the total microscopic energy which is only related with the translatory motion ψ_u^{mic} while the components of the couple stress tensor follow from the other portion of the total microscopic energy, related with micro rotations ψ_ω^{mic}.

The evolution of the macroscopic free energy can then be obtained applying the integral Eq.(21) to the evolution law of the microscopic free energy Eq.(23) as

$$\begin{aligned}\dot{\psi}^{mac}&=\frac{3}{2\pi}\int_\Omega\Big([\boldsymbol{T}^{sym}]^T\cdot\boldsymbol{\sigma}_T^{sym}-[\boldsymbol{T}^{skw}]^T\cdot\boldsymbol{\sigma}_T^{skw}+\\ &+\boldsymbol{N}\sigma_N\Big)\,d\Omega:\dot{\boldsymbol{\epsilon}}+\frac{3}{2\pi}\int_\Omega\Big(\boldsymbol{N}\mu_N+[\boldsymbol{T}^{sym}]^T\cdot\boldsymbol{\mu}_T^{sym}+\\ &-[\boldsymbol{T}^{skw}]^T\cdot\boldsymbol{\mu}_T^{skw}\Big)\,d\Omega:\dot{\boldsymbol{\kappa}}+\\ &-\frac{3}{2\pi}\int_\Omega(\mathcal{D}_u^{mic}+\mathcal{D}_\omega^{mic})d\Omega \quad (27)\end{aligned}$$

The macroscopic stress tensor and couple stress tensor are thus obtained from the microscopic constitutive stress and couple stress components as follows

$$\begin{aligned}\boldsymbol{\sigma}^t &= \tfrac{3}{2\pi}\int_\Omega \Big([\boldsymbol{N}\sigma_N + [\boldsymbol{T}^{sym}]^T\cdot\boldsymbol{\sigma}_T^{sym} \\ &\quad -[\boldsymbol{T}^{skw}]^T\cdot\boldsymbol{\sigma}_T^{skw}]\Big)\,d\Omega \qquad (28)\\ \boldsymbol{\mu}^t &= \tfrac{3}{2\pi}\int_\Omega \Big([\boldsymbol{N}\kappa_N + [\boldsymbol{T}^{sym}]^T\cdot\boldsymbol{\kappa}_T^{sym} \\ &\quad -[\boldsymbol{T}^{skw}]^T\cdot\boldsymbol{\kappa}_T^{skw}]\Big)\,d\Omega\end{aligned}$$

In order to satisfy the macroscopic dissipation inequality

$$\mathcal{D}^{mac} = \frac{3}{2\pi}\int_\Omega [\mathcal{D}_u^{mic} + \mathcal{D}_\omega^{mic}]d\Omega \geq 0 \qquad (29)$$

we will require that the total microscopic energy dissipation on every micro plane is non-negative

$$\mathcal{D}^{mic} = \mathcal{D}_u^{mic} + \mathcal{D}_\omega^{mic} \geq 0 \qquad (30)$$

which is a stronger requirement than that of Eq.(29) and therefore represents a sufficient condition to fulfill the second law of thermodynamics.

The evolution law of the microscopic free energy in Eq.(23) can be understood as the microscopic form of the Clausius-Duhem inequality for the isothermal case, which can be now rewritten as

$$\begin{aligned}\mathcal{D}^{mic} = \mathcal{D}_u^{mic} + \mathcal{D}_\omega^{mic} = \mathcal{P}_u^{mic} - \dot\psi_u^{mic} + \\ +\mathcal{P}_\omega^{mic} - \dot\psi_\omega^{mic} \geq 0 \qquad (31)\end{aligned}$$

with the microscopic stress and couple stress power

$$\begin{aligned}\mathcal{P}_u^{mic} &= \sigma_N\dot\epsilon_N + \boldsymbol{\sigma}_T^{sym}\cdot\dot{\boldsymbol{\epsilon}}_T^{sym} + \boldsymbol{\sigma}_T^{skw}\cdot\dot{\boldsymbol{\epsilon}}_T^{skw} \qquad (32)\\ \mathcal{P}_\omega^{mic} &= \mu_N\dot\kappa_N + \boldsymbol{\mu}_T^{sym}\cdot\dot{\boldsymbol{\kappa}}_T^{sym} + \boldsymbol{\mu}_T^{skw}\cdot\dot{\boldsymbol{\kappa}}_T^{skw}\end{aligned}$$

VI. MICRO POLAR-BASED MICRO PLANE ELASTICITY

In case of hiper-elasticity the free energy agrees with the stored energy which is assumed here to be composed by uncoupled membrane and bending contributions in the form

$$\begin{aligned}\psi_u^{mic} &= W_{Nu}(\epsilon_N) + W_{Tu}^{sym}(\boldsymbol{\epsilon}_T^{sym}) + W_{Tu}^{skw}(\boldsymbol{\epsilon}_T^{skw}) \qquad (33)\\ \psi_\omega^{mic} &= W_{N\omega}(\kappa_N) + W_{T\omega}^{sym}(\boldsymbol{\kappa}_T^{sym}) + W_{T\omega}^{skw}(\boldsymbol{\kappa}_T^{skw})\end{aligned}$$

whereby for linear elasticity the elastic moduli $E_{N\,u}$, $\mathbf{E}_{T\,u}^{sym}$, $\mathbf{E}_{T\,u}^{skw}$, $E_{N\,\omega}$, $\mathbf{E}_{T\,\omega}^{sym}$ and $\mathbf{E}_{T\,\omega}^{skw}$ were introduced into the microscopic energy functions as

$$\begin{aligned}W_{N\,u} &= \frac{1}{2}\epsilon_N E_{N\,u}\epsilon_N;\;\; W_{N\,\omega} = \frac{1}{2}\kappa_N E_{N\,\omega}\kappa_N\\ W_{T\,u}^{sym/skw} &= \frac{1}{2}\boldsymbol{\epsilon}_T^{sym/skw}\cdot\mathbf{E}_{T\,u}^{sym/skw}\cdot\boldsymbol{\epsilon}_T^{sym/skw} \qquad (34)\\ W_{T\,\omega}^{sym/skw} &= \frac{1}{2}\boldsymbol{\kappa}_T^{sym/skw}\cdot\mathbf{E}_{T\,\omega}^{sym/skw}\cdot\boldsymbol{\kappa}_T^{sym/skw}\end{aligned}$$

Hyper-elastic behavior of both the membrane and bending stiffness components is characterized by zero internal variables ($\boldsymbol{q}_u = \boldsymbol{q}_\omega \equiv \boldsymbol{0}$). Therefore, the microscopic free energy reduces to

$$\begin{aligned}\psi^{mic} = \psi_u^{mic}(\epsilon_N, \boldsymbol{\epsilon}_T^{sym}, \boldsymbol{\epsilon}_T^{skw}) + \\ +\psi_\omega^{mic}(\kappa_N, \boldsymbol{\kappa}_T^{sym}, \boldsymbol{\kappa}_T^{skw}) \qquad (35)\end{aligned}$$

The previous definition of the microscopic Clausius-Duhem inequality in Eq.(31) then leads to the microscopic constitutive stresses and couple stresses as thermodynamically conjugate variables to the strain and micro curvature components, respectively

$$\begin{aligned}\sigma_N &= \frac{\partial\psi_u^{mic}}{\partial\epsilon_N} = E_{N\,u}\epsilon_N;\;\; \mu_N = \frac{\partial\psi_\omega^{mic}}{\partial\kappa_N} = E_{N\,\omega}\kappa_N\\ \boldsymbol{\sigma}_T^{sym/skw} &= \frac{\partial\psi_u^{mic}}{\partial\boldsymbol{\epsilon}_T^{sym/skw}} = \boldsymbol{E}_{T\,u}^{sym/skw}\cdot\boldsymbol{\epsilon}_T^{sym/skw} \qquad (36)\\ \boldsymbol{\mu}_T^{sym/skw} &= \frac{\partial\psi_\omega^{mic}}{\partial\boldsymbol{\kappa}_T^{sym/skw}} = \boldsymbol{E}_{T\,\omega}^{sym/skw}\cdot\boldsymbol{\kappa}_T^{sym/skw}\end{aligned}$$

From the macroscopic version of the Clausius-Duhem inequality the macroscopic stress and couple stress tensors follow as functions of the microscopic components

$$\begin{aligned}\boldsymbol{\sigma}^t &= \frac{3}{2\pi}\int_\Omega [\boldsymbol{N}E_{N\,u}\epsilon_N + [\boldsymbol{T}^{sym}]^T\cdot\boldsymbol{E}_{T\,u}^{sym}\cdot\boldsymbol{\epsilon}_T^{sym}\\ &\quad -[\boldsymbol{T}^{skw}]^T\cdot\boldsymbol{E}_{T\,u}^{skw}\cdot\boldsymbol{\epsilon}_T^{skw}]d\Omega\\ \boldsymbol{\mu}^t &= \frac{3}{2\pi}\int_\Omega [\boldsymbol{N}E_{N\,\omega}\kappa_N + [\boldsymbol{T}^{sym}]^T\cdot\boldsymbol{E}_{T\,\omega}^{sym}\cdot\boldsymbol{\kappa}_T^{sym}\\ &\quad -[\boldsymbol{T}^{skw}]^T\cdot\boldsymbol{E}_{T\,\omega}^{skw}\cdot\boldsymbol{\kappa}_T^{skw}]d\Omega\end{aligned}$$

The last equation can alternatively be rewritten as

$$\begin{aligned}\boldsymbol{\sigma}^t &= \mathsf{E}_u : \boldsymbol{\epsilon} \qquad (37)\\ \boldsymbol{\mu}^t &= \mathsf{E}_\omega : \boldsymbol{\kappa}\end{aligned}$$

whereby the macroscopic membrane and bending constitutive moduli are defined as follows

$$\begin{aligned}\mathsf{E}_i = \frac{3}{2\pi}\int_\Omega [E_{Ni}\boldsymbol{N}\otimes\boldsymbol{N}]\,d\Omega + \\ +\frac{3}{2\pi}\int_\Omega \left[[\boldsymbol{T}^{sym}]^T\cdot\boldsymbol{E}_{Ti}^{sym}\cdot\boldsymbol{T}^{sym}\right]d\Omega + \\ +\frac{3}{2\pi}\int_\Omega \left[[\boldsymbol{T}^{skw}]^T\cdot\boldsymbol{E}_{T\,i}^{skw}\cdot\boldsymbol{T}^{skw}\right]d\Omega \qquad (38)\end{aligned}$$

with the subscript $i = u, \omega$.

Next, under the common assumption of micro plane isotropy the tangential strain and curvature vectors and the tangential stress and couple stress vectors remain parallel during the entire load history. Consequently, we consider the following simplification

$$\begin{aligned} \boldsymbol{\epsilon}_T^{sym} \parallel \boldsymbol{\sigma}_T^{sym} &\rightarrow \boldsymbol{E}_{T\,u}^{sym} = E_{Tu}^{sym}\,\boldsymbol{I} \\ \boldsymbol{\epsilon}_T^{skw} \parallel \boldsymbol{\sigma}_T^{skw} &\rightarrow \boldsymbol{E}_{T\,u}^{skw} = E_{Tu}^{skw}\,\boldsymbol{I} \\ \boldsymbol{\kappa}_T^{sym} \parallel \boldsymbol{\mu}_T^{sym} &\rightarrow \boldsymbol{E}_{T\,\omega}^{sym} = E_{T\omega}^{sym}\,\boldsymbol{I} \\ \boldsymbol{\kappa}_T^{skw} \parallel \boldsymbol{\mu}_T^{skw} &\rightarrow \boldsymbol{E}_{T\,\omega}^{skw} = E_{T\omega}^{skw}\,\boldsymbol{I} \end{aligned} \tag{39}$$

Assuming further that the constitutive moduli are independent from the orientation of the micro planes we arrive at

$$\begin{aligned} \mathsf{E}_i \;=\; & \frac{3}{2\pi}\Big\{E_{Ni}\int_\Omega \boldsymbol{N}\otimes\boldsymbol{N}d\Omega + \\ & E_{Ti}^{sym}\int_\Omega [\boldsymbol{T}^{sym}]^T\cdot\boldsymbol{T}^{sym}d\Omega + \\ & E_{Ti}^{skw}\int_\Omega [\boldsymbol{T}^{skw}]^T\cdot\boldsymbol{T}^{skw}d\Omega\Big\} \end{aligned} \tag{40}$$

The integration formulae (14) to (20) allow an analytical evaluation of the integrals in Eq.(41) to render

$$\begin{aligned} \mathsf{E}_i \;=\; & \left[\frac{3}{5}E_{Ni} - \frac{3}{5}E_{Ti}^{sym}\right]\boldsymbol{I}_{vol} + \\ & + \left[\frac{2}{5}E_{Ni}\frac{3}{5}E_{Ti}^{sym}\right]\mathsf{I}^{sym} + E_{Ti}^{skw}\,\mathsf{I}^{skw} \end{aligned} \tag{41}$$

The comparison of Eq. (41) with the general isotropic non symmetric elastic tensors for decoupled membrane-bending behavior

$$\begin{aligned} \mathsf{E}_u &= \alpha_1\mathsf{I}_{vol} + [\alpha_2+\alpha_3]\mathsf{I}^{sym} + [\alpha_2-\alpha_3]\mathsf{I}^{skw} \\ \mathsf{E}_\omega &= \beta_1\mathsf{I}_{vol} + [\beta_2+\beta_3]\mathsf{I}^{sym} + [\beta_2-\beta_3]\mathsf{I}^{skw} \end{aligned} \tag{42}$$

then leads finally to the identifications

$$\begin{aligned} &\alpha_1 = \frac{3}{5}E_{Nu} - \frac{3}{5}E_{Tu}^{sym};\;\; \alpha_2-\alpha_3 = E_{Tu}^{skw} \\ &\alpha_2+\alpha_3 = \frac{2}{5}E_{Nu} + \frac{3}{5}E_{Tu}^{sym};\;\; \beta_1 = \frac{3}{5}E_{N\omega} - \frac{3}{5}E_{T\omega}^{sym} \\ &\beta_2+\beta_3 = \frac{2}{5}E_{N\omega} + \frac{3}{5}E_{T\omega}^{sym};\;\; \beta_2-\beta_3 = E_{T\omega}^{skw} \end{aligned} \tag{43}$$

whereby $\alpha_1 := L$ and $\alpha_2+\alpha_3 := 2G$ are recognized as the common Lamé parameters, while $\alpha_2-\alpha_3 := 2G_c$ is the micro polar shear modulus which couples the skew-symmetric stress-strain components.

VII. MICRO POLAR-BASED MICRO PLANE ELASTOPLASTICITY

In this section the thermodynamically consistent formulation of the micro plane-based micro polar elastoplastic model is presented both for the general case and for the von Mises type model.

A. General Case

The elastoplastic type of micro polar continuum response behavior is characterized by the additive decomposition of the macroscopic total strain and curvature tensors into elastic and plastic contributions

$$\begin{aligned} \boldsymbol{\epsilon} &= \boldsymbol{\epsilon}_e + \boldsymbol{\epsilon}_p \\ \boldsymbol{\kappa} &= \boldsymbol{\kappa}_e + \boldsymbol{\kappa}_p \end{aligned} \tag{44}$$

The kinematic constraint assumption extends the applicability of the additive decomposition to the microscopic level. As a consequence, the total strain and curvature components at micro planes can be expressed as

$$\begin{aligned} \epsilon_N^{sym} &= \epsilon_{N\,e}^{sym} + \epsilon_{N\,p}^{sym} & \kappa_N &= \kappa_{N\,e} + \kappa_{N\,p} \\ \boldsymbol{\epsilon}_T^{sym} &= \boldsymbol{\epsilon}_{T\,e}^{sym} + \boldsymbol{\epsilon}_{T\,p}^{sym} & \boldsymbol{\kappa}_T^{sym} &= \boldsymbol{\kappa}_{T\,e}^{sym} + \boldsymbol{\kappa}_{T\,p}^{sym} \\ \boldsymbol{\epsilon}_T^{skw} &= \boldsymbol{\epsilon}_{T\,e}^{skw} + \boldsymbol{\epsilon}_{T\,p}^{skw} & \boldsymbol{\kappa}_T^{skw} &= \boldsymbol{\kappa}_{T\,e}^{skw} + \boldsymbol{\kappa}_{T\,p}^{skw} \end{aligned} \tag{45}$$

In the most general case the tensor of internal variables includes the plastic contributions of all the strain and curvature components at the micro planes

$$\boldsymbol{q} = \boldsymbol{q}(\epsilon_{Np}^{sym}, \boldsymbol{\epsilon}_{Tp}^{sym}, \boldsymbol{\epsilon}_{Tp}^{skw}, \kappa_{Np}, \boldsymbol{\kappa}_{Tp}^{sym}, \boldsymbol{\kappa}_{Tp}^{skw}, \xi^{mic}) \tag{46}$$

whereby the scalar internal variable ξ^{mic} accounts for the simplest isotropic hardening/softening response.

The microscopic free energy follows from the definition of the elastic free energy and of the microscopic free energy functions in equations (35), (34) and (34) as

$$\begin{aligned} \psi^{mic} = &W_{N\,u}(\epsilon_N - \epsilon_{N\,p}) + W_{T\,u}^{sym}(\boldsymbol{\epsilon}_T^{sym} - \boldsymbol{\epsilon}_{T\,p}^{sym}) + \\ &+ W_{T\,u}^{skw}(\boldsymbol{\epsilon}_T^{skw} - \boldsymbol{\epsilon}_{T\,p}^{skw}) + W_{N\,\omega}(\kappa_N - \kappa_{N\,p}) + \\ &+ W_{T\omega}^{sym}(\boldsymbol{\kappa}_T^{sym} - \boldsymbol{\kappa}_{T\,p}^{sym}) + W_{T\,\omega}^{skw}(\boldsymbol{\kappa}_T^{skw} - \boldsymbol{\kappa}_{T\,p}^{skw}) + \\ &+ \int_0^{\xi^{mic}} \phi^{mic}(\tilde{\xi}^{mic})d\tilde{\xi}^{mic} \end{aligned} \tag{47}$$

whereby the restricted form of isotropic hardening/softening behavior is taken into account by means of the term $\int_0^{\xi^{mic}} \phi^{mic}(\tilde{\xi}^{mic})d\tilde{\xi}^{mic}$.

The constitutive stresses and couple stresses at micro planes are then obtained from the evaluation of the microscopic Clausius-Duhem inequality

$$\begin{aligned} &\sigma_N = \frac{\partial\psi^{mic}}{\partial\epsilon_{Ne}} = E_{Nu}\,\epsilon_{N\,e},\;\; \mu_N = \frac{\partial\psi^{mic}}{\partial\kappa_{Ne}} = E_{N\,\omega}\kappa_{N\,e} \\ &\boldsymbol{\sigma}_T^{sym/skw} = \frac{\partial\psi^{mic}}{\partial\boldsymbol{\epsilon}_{Te}^{sym/skw}} = \boldsymbol{E}_{Tu}^{sym/skw}\cdot\boldsymbol{\epsilon}_{Te}^{sym/skw} \\ &\boldsymbol{\mu}_T^{sym/skw} = \frac{\partial\psi^{mic}}{\partial\boldsymbol{\kappa}_{Te}^{sym/skw}} = \boldsymbol{E}_{T\omega}^{sym/skw}\cdot\boldsymbol{\kappa}_{Te}^{sym/skw} \end{aligned} \tag{48}$$

The evolution of the internal variables is restricted by the inequality of the microscopic dissipation

$$\mathcal{D}^{mic} = \sigma_N \, \dot{\epsilon}_{N\,p} + \boldsymbol{\sigma}_T^{sym} \cdot \dot{\boldsymbol{\epsilon}}_{T\,p}^{sym} + \boldsymbol{\sigma}_T^{skw} \cdot \dot{\boldsymbol{\epsilon}}_{T\,p}^{skw} + \mu_N \, \dot{\kappa}_{N\,p} +$$
$$+ \boldsymbol{\mu}_T^{sym} \cdot \dot{\boldsymbol{\kappa}}_{T\,p}^{sym} + \boldsymbol{\mu}_T^{skw} \cdot \dot{\boldsymbol{\kappa}}_{T\,p}^{skw} - \phi^{mic} \, \dot{\xi}^{mic} \geq 0 \quad (49)$$

Thus, the yield function on each micro plane can be defined in the form

$$\Phi^{mic} = \varphi(\sigma_N, \boldsymbol{\sigma}_T^{sym}, \boldsymbol{\sigma}_T^{skw}, \mu_N, \boldsymbol{\mu}_T^{sym}, \boldsymbol{\mu}_T^{skw}) + \\ -\phi^{mic}(\xi^{mic}) \leq 0 \quad (50)$$

whereby the function φ of the microscopic constitutive stresses and couple stresses is characterized by the gradients

$$\begin{array}{ll} \nu_{N\,u} \doteq \partial\varphi / \partial\sigma_N & \nu_{N\,\omega} \doteq \partial\varphi/\partial\mu_N \\ \boldsymbol{\nu}_{T\,u}^{sym} \doteq \partial\varphi/\partial\boldsymbol{\sigma}_T^{sym} & \boldsymbol{\nu}_{T\,\omega}^{sym} \doteq \partial\varphi/\partial\boldsymbol{\mu}_T^{sym} \\ \boldsymbol{\nu}_{T\,u}^{skw} \doteq \partial\varphi/\partial\boldsymbol{\sigma}_T^{skw} & \boldsymbol{\nu}_{T\,\omega}^{skw} \doteq \partial\varphi/\partial\boldsymbol{\mu}_T^{skw} \end{array} \quad (51)$$

For the associated case the plastic strain and curvature evolution laws are obtained from the variational problem defined by the dissipation inequality (49) under consideration of the convexity condition and of the constraint (50). For the general non-associated case we postulate instead

$$\begin{array}{ll} \dot{\epsilon}_{N\,p} = \dot{\gamma}^{mic}\vartheta_{N\,u}, & \dot{\boldsymbol{\epsilon}}_{T\,p}^{sym/skw} = \dot{\gamma}^{mic}\boldsymbol{\vartheta}_{T\,u}^{sym/skw} \\ \dot{\kappa}_{N\,p} = \dot{\gamma}^{mic}\vartheta_{N\,\omega}, & \dot{\boldsymbol{\kappa}}_{T\,p}^{sym/skw} = \dot{\gamma}^{mic}\boldsymbol{\vartheta}_{T\,\omega}^{sym/skw} \\ & \dot{\xi}^{mic} = \dot{\gamma}^{mic} \end{array} \quad (52)$$

with the flow directions at each micro plane

$$\begin{array}{ll} \vartheta_{N\,u} = \partial\breve{\Phi}/\partial\sigma_N & \vartheta_{N\,\omega} = \partial\breve{\Phi}/\partial\mu_N \\ \boldsymbol{\vartheta}_{T\,u}^{sym} = \partial\breve{\Phi}/\partial\boldsymbol{\sigma}_T^{sym} & \boldsymbol{\vartheta}_{T\,\omega}^{sym} = \partial\breve{\Phi}/\partial\boldsymbol{\mu}_T^{sym} \\ \boldsymbol{\vartheta}_{T\,u}^{skw} = \partial\breve{\Phi}/\partial\boldsymbol{\sigma}_T^{skw} & \boldsymbol{\vartheta}_{T\,\omega}^{skw} = \partial\breve{\Phi}/\partial\boldsymbol{\mu}_T^{skw} \end{array} \quad (53)$$

in terms of the plastic multiplier $\dot{\gamma}^{mic}$ and of the gradients to the microscopic plastic potentials $\breve{\Phi}$.

The Kuhn-Tucker loading-unloading conditions as well as the consistency condition can be defined on each micro plane as

$$\Phi^{mic} \leq 0, \quad \dot{\gamma}^{mic} \geq 0, \quad \Phi^{mic}\,\dot{\gamma}^{mic} = 0, \quad \dot{\Phi}^{mic}\,\dot{\gamma}^{mic} = 0 \quad (54)$$

An explicit solution for the plastic multiplier can be obtained from the consistency condition

$$\dot{\gamma}^{mic} = \frac{1}{h}[\nu_{Nu}E_{Nu}\boldsymbol{N} + \boldsymbol{\nu}_{Tu}^{sym} \cdot \boldsymbol{E}_{Tu}^{sym} \cdot \boldsymbol{T}^{sym} \\ -\boldsymbol{\nu}_{Tu}^{skw} \cdot \boldsymbol{E}_{Tu}^{skw} \cdot \boldsymbol{T}^{skw}] : \dot{\boldsymbol{\epsilon}} + \frac{1}{h}[\nu_{N\omega}E_{N\omega}\boldsymbol{N} \\ +\boldsymbol{\nu}_{T\omega}^{sym} \cdot \boldsymbol{E}_{T\omega}^{sym} \cdot \boldsymbol{T}^{sym} - \boldsymbol{\nu}_{T\omega}^{skw} \cdot \boldsymbol{E}_{T\omega}^{skw} \cdot \boldsymbol{T}^{skw}] : \dot{\boldsymbol{\kappa}} \quad (55)$$

whereby

$$h = H^{mic} + \nu_{Nu}E_{Nu}\vartheta_{Nu} + \boldsymbol{\nu}_{Tu}^{sym} \cdot \boldsymbol{E}_{Tu}^{sym} \cdot \boldsymbol{\vartheta}_{Tu}^{sym} \\ -\boldsymbol{\nu}_{Tu}^{skw} \cdot \boldsymbol{E}_{Tu}^{skw} \cdot \boldsymbol{\vartheta}_{Tu}^{skw} + \nu_{N\omega}E_{N\omega}\vartheta_{N\omega} \\ +\boldsymbol{\nu}_{T\omega}^{sym} \cdot \boldsymbol{E}_{T\omega}^{sym} \cdot \boldsymbol{\vartheta}_{T\omega}^{sym} - \boldsymbol{\nu}_{T\omega}^{skw} \cdot \boldsymbol{E}_{T\omega}^{skw} \cdot \boldsymbol{\vartheta}_{T\omega}^{skw} \quad (56)$$

and

$$H^{mic} = \frac{\partial\phi^{mic}(\xi^{mic})}{\partial\xi^{mic}} \quad (57)$$

Finally, the macroscopic elastoplastic constitutive equations can be expressed as

$$\begin{bmatrix} \dot{\boldsymbol{\sigma}}^t \\ \dot{\boldsymbol{\mu}}^t \end{bmatrix} = \begin{bmatrix} \mathsf{E}_{ep}^{u,u} & \mathsf{E}_{ep}^{u,\omega} \\ \mathsf{E}_{ep}^{\omega,u} & \mathsf{E}_{ep}^{\omega,\omega} \end{bmatrix} : \begin{bmatrix} \dot{\boldsymbol{\epsilon}} \\ \dot{\boldsymbol{\kappa}} \end{bmatrix} \quad (58)$$

with the elastoplastic operators

$$\begin{aligned} \mathsf{E}_{ep}^{u,u} &= \mathsf{E}_u - \frac{3}{2\pi}\int_\Omega \frac{1}{h}\tilde{\boldsymbol{n}}_u \otimes \tilde{\boldsymbol{m}}_u d\Omega \quad (59) \\ \mathsf{E}_{ep}^{\omega,\omega} &= \mathsf{E}_\omega - \frac{3}{2\pi}\int_\Omega \frac{1}{h}\tilde{\boldsymbol{n}}_\omega \otimes \tilde{\boldsymbol{m}}_\omega d\Omega \\ \mathsf{E}_{ep}^{u,\omega} &= -\frac{3}{2\pi}\int_\Omega \frac{1}{h}\tilde{\boldsymbol{n}}_u \otimes \tilde{\boldsymbol{m}}_\omega d\Omega \\ \mathsf{E}_{ep}^{\omega,u} &= -\frac{3}{2\pi}\int_\Omega \frac{1}{h}\tilde{\boldsymbol{n}}_\omega \otimes \tilde{\boldsymbol{m}}_u d\Omega \end{aligned}$$

whereby the modified gradients are defined as

$$\tilde{\boldsymbol{n}}_i = E_{Ni}\nu_{Ni}\boldsymbol{N} + \boldsymbol{T}^{sym} \cdot [\boldsymbol{E}_{Ti}^{sym} \cdot \boldsymbol{\nu}_{Ti}^{sym}] \\ -\boldsymbol{T}^{skw} \cdot [\boldsymbol{E}_{Ti}^{skw} \cdot \boldsymbol{\nu}_{Ti}^{skw}] \quad (60)$$

$$\tilde{\boldsymbol{m}}_i = E_{Ni}\vartheta_{Ni}\boldsymbol{N} + \boldsymbol{T}^{sym} \cdot [\boldsymbol{E}_{Ti}^{sym} \cdot \boldsymbol{\vartheta}_{Ti}^{sym}] \\ -\boldsymbol{T}^{skw} \cdot [\boldsymbol{E}_{Ti}^{skw} \cdot \boldsymbol{\vartheta}_{Ti}^{skw}] \quad (61)$$

with the subscript $i = u, \omega$.

Remark: the resulting format of the micro polar micro plane elastoplastic tangent operator is quite similar to that of the classical micro polar model (compare Willam *et al.* (1995)) with exception of the integrals which account for the microscopic contribution to the macroscopic operator in case of the micro polar micro plane formulation.

B. Von Mises Type Model

The classical micro polar elastoplastic von Mises type model, see e.g. de Borst (1991), is characterized by the yield condition

$$\Phi^{mac} = \sqrt{3J_2} - \phi^{mac} = 0 \quad (62)$$

$$J_2 = \frac{1}{4}\boldsymbol{s} : \boldsymbol{s} + \frac{1}{4}\boldsymbol{s} : \boldsymbol{s}^t + \frac{1}{2l_c^2}\boldsymbol{\mu} : \boldsymbol{\mu} \quad (63)$$

with $\boldsymbol{s}$ the deviator of $\boldsymbol{\sigma}$ and with yield stress with linear hardening

$$\phi^{mac} = \phi_0^{mac} + H^{mac}\xi^{mac} \quad (64)$$

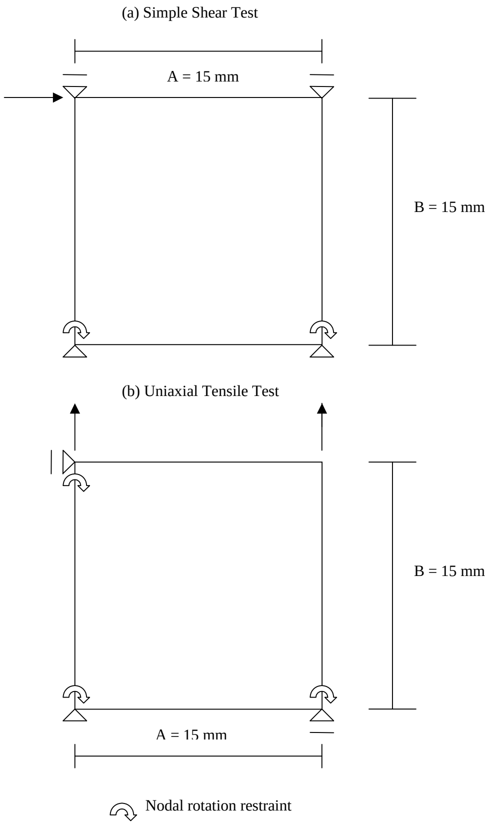

Figure 2: Boundary conditions. Plane strain axial extension and simple shear tests.

Here the evolution of the hardening-softening parameter is given by

$$\dot{\xi}^{mac} = \{\frac{1}{3}\dot{\boldsymbol{\epsilon}}_p : \dot{\boldsymbol{\epsilon}}_p + \frac{1}{3}\dot{\boldsymbol{\epsilon}}_p : \dot{\boldsymbol{\epsilon}}_p^t + \frac{2}{3}l_c^2 \dot{\boldsymbol{\kappa}}_p : \dot{\boldsymbol{\kappa}}_p\}^{1/2} = \dot{\gamma}^{mac} \quad (65)$$

Assuming that the second invariant of the stress deviator tensor s is a function of the tangential stress vectors and of the tangential couple stress vectors of the micro planes, the von Mises yield condition at the micro plane level can be expressed in the format

$$\Phi^{mic} = \{\boldsymbol{\sigma}_T^{sym} \cdot \boldsymbol{\sigma}_T^{sym} + \boldsymbol{\sigma}_T^{skw} \cdot \boldsymbol{\sigma}_T^{skw} \frac{1}{l_c^2} + [\boldsymbol{\mu}_T^{sym} \cdot \boldsymbol{\mu}_T^{sym} + \boldsymbol{\mu}_T^{skw} \cdot \boldsymbol{\mu}_T^{skw}]\}^{1/2} - \phi^{mic} \leq 0 \quad (66)$$

with the yield stress with linear hardening

$$\phi^{mic} = \phi_0^{mic} + H^{mic}\xi^{mic} \quad (67)$$

Here the evolution of the hardening-softening parameter is given by

$$\dot{\xi}^{mic} = \{\dot{\boldsymbol{\epsilon}}_{Tp}^{sym} \cdot \dot{\boldsymbol{\epsilon}}_{Tp}^{sym} + \dot{\boldsymbol{\epsilon}}_{Tp}^{skw} \cdot \dot{\boldsymbol{\epsilon}}_{Tp}^{skw} + l_c^2[\dot{\boldsymbol{\kappa}}_{Tp}^{sym} \cdot \dot{\boldsymbol{\kappa}}_{Tp}^{sym} + \dot{\boldsymbol{\kappa}}_{Tp}^{skw} \cdot \dot{\boldsymbol{\kappa}}_{Tp}^{skw}]\}^{1/2} = \dot{\gamma}^{mic} \quad (68)$$

which, similarly to the macroscopic description, coincides with the plastic multiplier.

VIII. NUMERICAL ANALYSIS

In this section we analyze the predictions of the micro polar micro plane elastoplastic von Mises model for the uniaxial tensile and simple shear tests. Fig. 2 illustrates the boundary conditions of these tests which were analyzed under plane strain constraints. In both one element meshes of Fig. 2 the standard bilinear quadrilateral finite element with four integraion points was used. This finite element formulation of micro polar continuum problems is obtained by means of discretizations of the weak form of the balance equations in the spirit of the Dirichlet variational principle, see Willam et al. (1995). Thereby the displacements and rotations (and their variations) are approximated by the same shape functions according to the Galerkin-Bubnov method.

In the simple shear test, full displacement and rotation restraint were considered on the nodes located on the bottom of the quadrilateral element while only the vertical displacements were restrained on the other element nodes. On the other hand, in case of the axial extension test, the full displacement and rotation restraint were assumed only in one element node as indicated in Fig. 2 while in other two nodes one displacement possibility together with the in plane rotation were restrained according to the double symmetry of the problem. Both, the yield condition and hardening/softening evolution law are those indicated in section VII.B. The micro polar elastic parameters at micro planes for the numerical analysis were obtained according to the equations in section 6 so that the overall Young's modulus is $E = 30000\,N/mm^2$, the Poisson's ratio $\nu = 0.2$, the micro polar shear modulus $G_c = G$ and the characteristic length $l_c = 1mm$. Following the equations (43) we obtain: $E_{Nu} = 33333.33$, $G = 12500$, $E_{Tu}^{sym} = 19444.45$, $E_{Tu}^{skw} = 25000$, $E_{N\omega} = E_{T\omega}^{sym} = E_{T\omega}^{skw} = 25000$.

The non-symmetric stress field in the case of a micro polar continuum and the resulting complex form of the second invariant J_2 avoids an analytical procedure to obtain the relationship between the microscopic and macroscopic von Mises stresses ϕ_0^{mic} and ϕ_0^{mac}, respectively. As a consequence and for the purpose of the numerical analyses in this work, these stresses were chosen so that similar predictions of the J_2 type maximum strength cor-

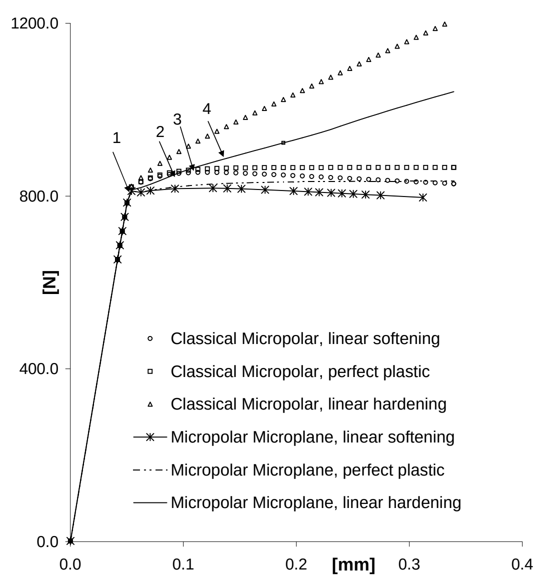

Figure 3: Prediction of the axial extension test.

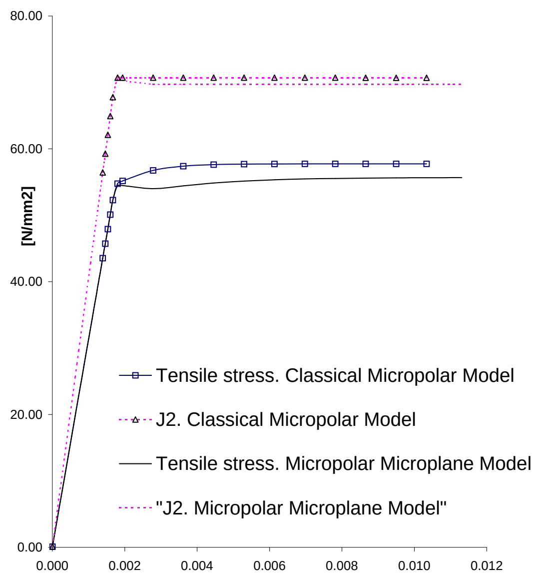

Figure 5: Stress-strain prediction of the axial extension test.

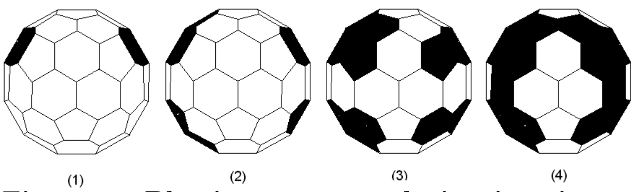

Figure 4: Plastic process evolution in micro planes. Axial extension test

responding to both the uniaxial tensile and simple shear tests are obtained with the microscopic and the macroscopic micro polar models. From this numerical calibration the resulting values are $\phi_0^{mic} = 23.5\ N/mm^2$ and $\phi_0^{mac} = 50.0\ N/mm^2$ for the axial extension test while these stresses are $\phi_0^{mic} = 29.0\ N/mm^2$ and $\phi_0^{mac} = 50.0\ N/mm^2$ for the simple shear test.

A. Axial Extension Test

Fig. 3 illustrates the numerical predictions of the uniaxial tensile test with the micro polar micro plane elastoplastic model and with the classical micro polar elastoplastic model. Three different types of evolution laws of the stress functions ϕ^{mic} and ϕ^{mac} were considered for these models, corresponding to perfect plasticity, linear hardening and linear softening behavior. The first observation from the comparison between the predictions of both types of micro polar models is that their response behaviors during the elastic range agree very well. Also the overall predictions of both models in the plastic range under linear softening and perfect plasticity are very similar. However, under linear hardening assumption the classical micro plane model leads to a much more ductile response behavior indicating that this formulation is more sensitive to variations of the hardening evolution law.

The microscopic model allows a much more detailed analysis of the failure mechanism and evolution as can be observed in Fig. 4 which shows the spatial development of the plastic process in the case of the axial extension test predicted by the micro polar micro plane model with linear hardening. Each diagram in this figure corresponds to the load step indicated in the load-displacement curve (compare Fig. 3). During the load history, a tendency towards texture evolution can be recognized. Under uniaxial tension, the plastic behavior develops in the planes located under an angle of about 45^o towards the loading axis in the loading plane. Similar effects were

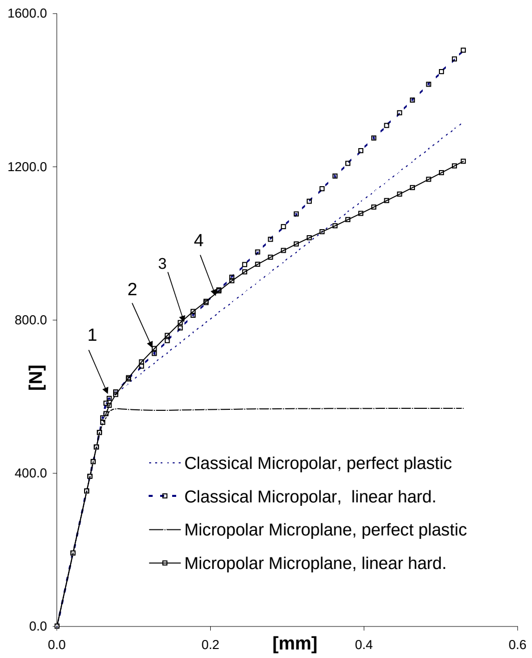

Figure 6: Prediction of the simple shear test.

observed by Kuhl *et al.* (2001) in the uniaxial tensile test's predictions obtained with the micro plane elastoplastic model for the classical Boltzmann continuum. We analyze now the fundamental differences between the numerical predictions of the micro polar micro plane and of the classical micro polar model with perfect plasticity in Fig. 3. In the case of the classical micro polar model with perfect plasticity the requirement for constant values of J_2 due to the yield condition

$$\Phi^{mac} = \sqrt{3J_2} - \phi_0^{mac} = 0 \qquad (69)$$

is responsible for the plateau in the J_2 evolution which immediately follows the elastic response, as indicated in Fig. 5. On the other hand, the evolution of the the axial tensile force as well as that of the vertical tensile stress in Fig. 3 and Fig. 5, respectively, show a smooth transition from the elastic to the perfect plastic regime.

The micro polar micro plane model with perfect plasticity leads to a macroscopic stress tensor's evolution during the axial extension test characterized by an initial smooth softening response of J_2 and subsequent plateau.

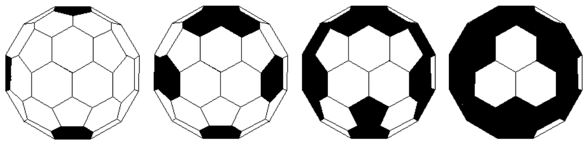

Figure 7: Plastic process evolution in micro planes. Simple shear test.

The same response behavior is observed in the evolutions of the vertical tensile stress in Fig. 5 and of the axial force in Fig. 3.

B. Simple Shear Test

The numerical predictions of the micro polar micro plane model for the simple shear test and the comparison with the corresponding predictions of the classical micro polar model are indicated in Fig. 6. Both a linear hardening and a perfect plastic evolution laws were assumed for ϕ^{mic} and ϕ^{mac} in equations (64) and (67), corresponding to the micro plane model and to the macroscopic model, respectively. It is important to note that in the simple shear test, contrarily to the axial extension test, the microrotations are activated.

Fig. 7 illustrates the development of failure predicted by the micro polar micro plane model with linear hardening. Again, a tendency towards texture evolution can be recognized. However, in the case of the simple shear test, the inelastic deformation process takes place in the upper, lower, left and right micro plane. This strong failure distribution in micro planes explains the more ductile behavior of the simple shear test predicted by the micro plane micro polar model when compared to the corresponding predictions of the uniaxial tensile test. The results in Fig. 6 also indicate that the micro polar micro plane model with perfect plasticity leads, as expected, to a plateau of the external shear force. However, this is not the case of the classical Cosserat model which leads to continuous hardening of the external shear force although perfect plasticity was considered. This is due to the evolution of the nonuniform microrotations which are activated in this test.

IX. CONCLUSIONS

In this work the thermodynamically consistent approach for deriving micro plane constitutive formulations by Carol *et al.* (2001) and Kuhl *et al.* (2001) was reformulated for elastic and inelastic micro polar continua. As in the previous work, the main assumption is the incorporation of a microscopic free Helmholtz energy on every micro plane, which in the present case includes the contributions of the additional degree of freedom and stiffness of the micro polar continuum, represented by the micro rotations and the couple stresses. Moreover, an uncoupled format of the free energy in terms of the membrane and bending contributions is considered.

From the resulting constitutive equations for the micro polar micro plane elastic model an explicit solution for the characteristic length was obtained in terms of the ratio between the bending elastic moduli and the micro polar shear modulus. The solutions for the micro polar micro plane elastoplastic model include the macroscopic explicit formulation of the constitutive tangential moduli in terms of the microscopic contributions. The general elastoplastic formulation for the micro polar micro plane model was particularized for von Mises type elastoplasticity.

The numerical results in this work show the predictions of the J_2 elastoplastic model for the uniaxial tensile and simple shear tests. Also the main differences with the corresponding predictions of the classical micro polar elastoplastic model were highlighted.

The proposed constitutive theory allows the formulation of models based on relevant aspects of the material microstructure which exceeds the capacity of the theoretical framework developed so far for the prediction of anisotropic response behaviors.

REFERENCES

Batdorf,S., B.Budiansky. "A mathematical theory of plasticity based on the concept of slip." Tech.Note 1871.*N.A.C.A.*. 1949.

Bazant,Z."Imbricate Continuum and its Variational Derivation."*J.E.Mech.*,110,pp.1693-1712. 1984.

Bazant, Z.P., P.G. Gambarova. "Crack shear in concrete: Crack band micro plane model." *J. Struct. Eng.*, ASCE, 110,pp.2015-2036. 1984.

Bazant,Z.,B.Oh."Micro plane model for progressive fracture of concrete and rock." *J.E.Mech.*, 111, pp.559-582. 1985.

Bazant,Z.,B.Oh. "Efficient numerical integration on the surface of a sphere." *ZAMM*, 66(1),pp.37-49. 1986.

Bazant,Z.,P.Prat."Micro plane model for brittle plastic material: Part I & II." *J.E.Mech.*, 114,pp.1672-1702. 1988.

Carol,I.,Z.Bazant,P.Prat. "Geometric damage tensor based on micro plane model." *J.E.Mech.*, 117,pp.2429-2448. 1991.

Carol,I., Z.Bazant,P.Prat. "New explicit micro plane model for concrete: Theoretical aspects and numerical implementation."*I.J.S.& Struc.*,29,pp.1173-1191. 1992.

Carol,I.,Z.Bazant. "Damage and plasticity in micro plane theory." *I.J.S.& Struc.*, 34, pp.3807-3835. 1997.

Carol,I.,M.Jirasek,Z.Bazant. "A thermodynamically consistent approach to micro plane theory. Part I." *Int.J.S. & Struc.*, 38,pp.2921-2931. 2001.

Cosserat,E.,F.Cosserat. "Theory des corps deformables." *Herman et fils*, Paris.1909.

de Borst,R. "Simulation of strain localization: A reappraisal of the Cosserat Continuum." *Eng.Comp.*,8,pp.317-332. 1991.

Eringen,A."Theory of micro polar Elasticity."*Fracture, an Adv.Treatise*.Ed.L.Liebowitz, Ac.Press.1968.

Kuhl,E.,P.Steinmann,I.Carol. "A thermodynamically consistent approach to micro plane theory. Part II." *Int.J.S.& Struc.*,38,pp.2933-2952. 2001.

Lubarda,V.,D.Krajcinovic."Damage tensors and the crack density distribution." *Int.J.S. & Struc.*, 30,pp.2859-2877. 1993.

Mühlhaus,H. "Application of Cosserat theory in numerical solutions of limit load problems."*Ing.Archive*,59,pp. 124-137. 1989.

Sluys,P. *Wave propagation, localization and dispersion in softening solids*. Dissertation, Delft Univ.of Tech.,Delft.1992.

Steinmann,P.,K. Willam. "Localization within the framework of micro polar elastoplasticity." *60th Anniv.Vol.Prof. Lippmann*, V.Mannl,O.Brueller,J.Najar (eds.), Springer Verlag,pp.296-313. 1991.

Taylor,G. "Plastic strain in metals." *J. Inst. Metals*,62,pp.307-324. 1938.

Willam,K.,A.Dietsche. "Regularization of localized failure computations." *COMPLAS III*. Edt. E.Onate, E.Hinton, R.Owen, Pineridge Press,pp.2185-2204. 1992.

Willam, K., A. Dietsche, M. Iordache, P. Steinmann. "Localization in Micro polar Continua." *Cont.Models for Materials with Microstructure*. Ed. H. Mühlhaus. J.Wiley & Sons Ltd., pp. 297-339. 1995.

Received: October 15, 2003.
Accepted for publication: April 15, 2004.
Recommended by Subject Editor: E. Dvorkin.